WiHlo: A Case Study of WiFi-Based Human Passive Localization by Angle Refinement

Zengshan Tian, Weiqin Yang(✉), Yue Jin, and Gongzhui Zhang

School of Communication and Information Engineering,
Chongqing University of Posts and Telecommunications,
Chongqing 400065, China
yangweiqin555@gmail.com

Abstract. The emergence of the Internet of Things (IoT) has promoted the interconnection of all things. And the access control of devices and accurate service promotion are inseparable from the acquisition of location information. We propose WiHlo, a passive localization system based on WiFi Channel State Information (CSI). WiHlo directly estimates the human location by refining the angle-of-arrival (AoA) of the subtle human reflection. WiHlo divides the received signals into static path components and dynamic path components, and uses phase offsets compensation and direct wave suppression algorithms to separate out the dynamic path signals. By combining the measured AoAs and time-of-arrivals (ToAs) with Gaussian mean clustering and probability analysis, WiHlo identifies the human reflection path from the dynamic paths. Our implementation and evaluation on commodity WiFi devices demonstrate WiHlo outperforms the state-of-the-art AoA estimation system in actual indoor environment.

Keywords: WiFi · Passive localization · AoA

1 Introduction

Indoor localization systems play an increasingly important role in many emerging applications, such as indoor navigation, body/behavioral analysis, aged care and unobtrusive motion tracking, etc. In the last few decades, indoor localization systems based on mobile phones, wearable devices, and camera have been proposed. However, all of these technologies require the target to be actively involved

This work is supported in part by National Natural Science Foundation of China (61771083, 61704015), the Program for Changjiang Scholars and Innovative Research Team in University (IRT1299), Special Fund of Chongqing Key Laboratory (CSTC), Fundamental and Frontier Research Project of Chongqing (cstc2017jcyjAX0380), and University Outstanding Achievement Transformation Project of Chongqing (KJZH17117).

H. Gao et al. (Eds.): ChinaCom 2019, LNICST 313, pp. 216–229, 2020.
https://doi.org/10.1007/978-3-030-41117-6_18

in the location process in a device-carrying manner, which we call device-based localization [1–3]. The localization method that the target needs to carry devices at all times is actually not feasible in reality. In the scenario where users take the initiative to obtain location information, such as family life track tracking and hospital health monitoring, it is against users' habits to require a person to wear a variety of unfamiliar devices, and even they often forget to wear relevant devices. In the localization of fire rescue, it is impossible for us to require firefighters to carry a large number of professional equipment, and the masses waiting for rescue are usually not carrying any localization equipment. The limitations of the above scenarios lead to the emergence of passive localization, which arouses people's interest in this field.

Passive localization technologies based on ultrasonic, radar, and computer vision have all been studied for years. However, ultrasonic-based localization systems have a small coverage area and significantly reduced performance in a noisy environment [4]. Radar-based systems require very high bandwidth and the costs are expensive [5]. Computer vision-based systems can only work in bright Line-of-sight (LOS) environments and the privacy of users is not protected [6]. With the development of WiFi technology, many indoor scenes can install high-speed and stable WiFi infrastructures. These devices have low cost and large coverage. Compared with other systems, WiFi based passive localization systems have better application prospects.

In this work, we aim to achieve accurate passive human localization using WiFi Channel State Information (CSI). While passive localization with only commodity WiFi infrastructures is challenging. In these systems, the received signals are superposition of direct path signals, static objects reflection signals and moving human reflection signal, and the energy exponent of human reflection signal we care about is far weaker than those strong reflections. And due to the imperfection of the hardware and the non-strict synchronization of the transceivers, there are different offsets in phase measurements. Therefore, it is difficult to extract useful information from the aliasing signal.

We propose WiHlo, which can get an accurate location information of human by angle-of-arrival (AoA) refinement. The main contributions of our work are summarized as follows:

- A Two-dimensional Spatial Smoothing (2D-SS) algorithm is applied to construct a large-scale virtual antenna arrays for super-resolution estimation of time of arrival (ToA) and AoA.
- We separate out the dynamic path signal from the aliasing signal through our dynamic path capture algorithm. And we introduce the Gaussian mean clustering and probability analysis to identify the human reflection path's AoA.
- We conduct comprehensive field studies to evaluate the performance of WiHlo. The experimental results show that WiHlo achieves a median localization error of 0.67 m in actual indoor environment using only two receivers, which is better than the state-of-the-art AoA based system.

The rest of the paper is organized as follows. Section 2 gives the related work. Section 3 describes the system design. Section 4 validates system's performance with the experimental evaluations. The conclusion is drawn in Sect. 5.

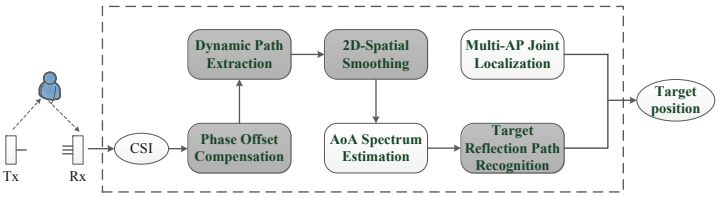

Fig. 1. System architecture: WiHlo consists of four main components. Once we get the AoA measurement on multiple receivers, we can obtain the location of the human using the triangulation algorithm.

2 Related Work

Our work is closely related to the research of indoor localization. We will discuss the related work in following two groups: Non-WiFi-based and WiFi-based approaches.

Non-WiFi-based indoor localization technology mainly includes Zigbee [24,25] and Bluetooth [26,27]. Zigbee is a wireless network protocol based on IEEE 802.15.4 for low-speed and short-distance transmission. It has the advantages of low complexity, short distance, low cost and low power consumption, etc. However, due to the characteristics of its own gateway attribute, the technology has high latency, short distance and other congenital defects when applied to localization work. Bluetooth localization technology (BLE) is also a research hotspot in recent years, especially the low power consumption Bluetooth 4.0 has more advantages of energy saving, low cost, low latency, and long effective connection distance. When the device enters the signal coverage area, the corresponding application will detect the received Bluetooth signal and use it to locate or forward information. BLE is mainly subject to the limited propagation distance, so in order to achieve a wide range of localization requirements, we usually need to deploy a large number of anchor devices.

In order to achieve high bandwidth and high quality Wireless Local Area Network (WLAN) services and make WLAN reach the performance level of Ethernet, experts at home and abroad have been devoting themselves to the research of new standards. The WLAN protocol 802.11n, which is officially approved by the IEEE, is an industry-changing protocol, and its modulation method is orthogonal frequency division multiplexing (OFDM). In the indoor channel research, the channel state information (CSI) of each subcarrier channel can be parsed by this technology, which makes it possible for ordinary academic personnel to conduct finer channel characteristics research through WLAN.

We divide WiFi based indoor localization technologies into the pattern-based and the model-based approaches. The pattern-based approaches work by selecting and learning features. Xiao et al. [20] use the frequency diversity feature of CSI to build a fingerprint database, achieve DFL on commodity WiFi devices by monitoring the CSI feature pattern shift. Seifeldin et al. [21] develop Nuzzer, it builds a passive radio map in the area of interest for large-scale localization. When faced with general perception, pattern-based approach achieves the expected results. However, when the perception task and perception environment are more complex, the performance of these systems declined significantly. The model-based approach is to understand and abstract the mathematical model between the received signal and target location. Li et al. [8] propose MaTrack, it utilizes the CSI subcarrier phase measurements to identify the moving target's angle information, and with only two receivers it achieves a high accuracy. Wang et al. [19] propose LiFS, this system utilizes Fresnel model to improve the accuracy of localization in LOS scenarios. In this work, we aim to use AoA model to achieve passive human localization. To distinguish from prior works, we focus on better extracting the subtle human reflection signals and obtain a refined AoA estimate.

3 System Design

3.1 System Overview

In this section, we present the detailed design of WiHlo. As shown in Fig. 1, our system is composed of four main components, namely Phase Offset Compensation, Dynamic Path Extraction, 2D-Spatial Smoothing, and Target Reflection Path Recognition. In following sections, we will show details of each component.

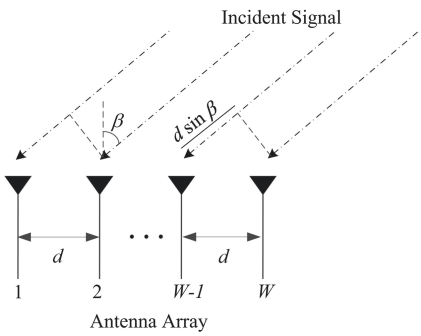

Fig. 2. A linear array with W antennas at the receiver. The incident angle of the signal is β, antenna spacing d is half-wavelength of the signal.

3.2 AoA Estimation Algorithm Based on 2D-SS

As shown in Fig. 2, we place W antennas with the antenna spacing of size d on the receiver, where d is half-wavelength of the signal. Therefore, the distance difference between the two adjacent antennas on the array is $dsin\beta$. It can be deduced from the distance difference that the phase difference between antennas with W-1 antenna spacing is $-2\pi f\left(W-1\right)d\sin\beta/c$, where f is the signal frequency and c is the speed of light. The introduced phase difference on two adjacent antennas can be written as a function of the AoA

$$\psi_{\beta}{=}e^{-j2\pi fd\sin(\beta)/c} \tag{1}$$

To achieve super-resolution estimation of AoA, we do not only introduce phase differences across antennas but also introduce phase differences across subcarriers, as described in [3]. The time differences introduce measurable phase differences across subcarriers, for evenly-spaced subcarriers, the phase difference introduced across two adjacent subcarriers is $-2\pi f_{\sigma}\tau$, where f_{σ} is the adjacent subcarrier spacing and τ is the ToA. The introduced phase difference across subcarriers can be written as a function of the ToA of the path:

$$\Theta\left(\tau_i\right)=e^{-j2\pi f_{\sigma}\tau_i} \tag{2}$$

where τ_i is the ToA of the ith propagation path. Thus, for W antennas and K subcarriers, we obtain a total of $W\times K$ virtual sensors. For a path with AoA β and ToA τ, the steering vector can be rewritten as:

$$\mathbf{v}\left(\beta,\tau\right)=\left[1,\cdots,\Theta\left(\tau\right)^{K-1},\cdots,{\psi_{\beta}}^{W-1},\cdots,{\psi_{\beta}}^{W-1}\Theta\left(\tau\right)^{K-1}\right]^{T} \tag{3}$$

Assume there are L incident signals and the received signal of lth path for the first subcarrier of first antenna is $s_l\left(t\right)$, the received signal at each sensor is a superposition of all paths and can be expressed as:

$$\mathbf{U}\left(t\right)=\left[u_1\left(t\right),\cdots,u_M\left(t\right)\right]^{T}=\sum_{l=1}^{L}\mathbf{v}\left(\beta_l\right)s_l\left(t\right)+\mathbf{N}\left(t\right)=\mathbf{DS}\left(t\right)+\mathbf{N}\left(t\right) \tag{4}$$

where β_l represents the AoA of the lth incident signal, $\mathbf{D}$ is the direction matrix, $\mathbf{N}\left(t\right)$ is the noise vector. The basic idea of the MUSIC algorithm [7] is eigenstructure analysis of an $W\times W$ correlation matrix $\mathbf{R}_U$ of the W CSI samples. From (4), we represent the covariance matrix as:

$$\mathbf{R}_U=\mathbb{E}\left[\mathbf{UU}^{\mathrm{H}}\right]=\mathbf{D}\mathbb{E}\left[\mathbf{UU}^{\mathrm{H}}\right]\mathbf{D}^{\mathrm{H}}+\mathbb{E}\left[\mathbf{NN}^{\mathrm{H}}\right]=\mathbf{DR}_S\mathbf{D}^{\mathrm{H}}+\sigma^2\mathbf{I} \tag{5}$$

where $\mathbf{R}_S$ is the correlation matrix of the signal vector, $\mathbf{I}$ is an identity matrix and σ^2 is the variance of noise, $\left(\cdot\right)^H$ denote conjugate operation.

By doing eigenvalue decomposition on the covariance matrix $\mathbf{R}_U$, we can get W eigenvalues. The largest L eigenvalues correspond to the L path signals and the other W-L eigenvalues correspond to the noise. And we have a eigenvectors corresponding to the smallest W-L eigenvalues called noise subspace

$\mathbf{E}_{\mathrm{N}} = [\overrightarrow{e}_1, \cdots, \overrightarrow{e}_{W-L}]$. Since the signal and the noise subspace are orthogonal, so the AoA spectrum function can be expressed as:

$$P(\beta)_{MUSIC} = \frac{1}{\mathbf{v}^{\mathrm{H}}(\beta)\,\mathbf{E}_{\mathrm{N}}\mathbf{E}_{\mathrm{N}}{}^{\mathrm{H}}\mathbf{v}(\beta)} \tag{6}$$

where $\mathrm{v}(\beta)$ is called the steering vector, in which sharp peaks occur at the AoAs of the target reflective signals.

In indoor environment, there are strong direct and multipath interference signals, and they have coherence with the human reflection signals. To eliminate the interference of the coherent signals and tackle the limitation of insufficient number of antennas, we conduct the 2D-SS [11,12] on $\mathbf{R}_U$ instead of $\mathbf{U}(t)$. 2D-SS is a kind of spatial smoothing technology, it is an effective method to deal with coherent or strongly coherent signals. Its basic idea is to divide the isometric linear array into several overlapping sub-arrays, so that the rank of the antenna array model is only related to the direction of arrival of the signal, but not affected by signal correlation, so as to achieve the purpose of de-correlation. We give a schematic diagram of Fig. 3 to illustrate the application of 2D-SS, the elements in the dashed blue and red boxes construct the covariance matrices of the first and second sub-arrays. Based on the observation that the first elements of the covariance matrices of the first and second sub-arrays are $h_{1,1} \times h_{1,1}$ and $h_{1,2} \times h_{1,2}$, we get the covariance matrices of the existing sub-arrays by increasing the subcarrier ID and antenna index number to $P_2 = 30 - L_{sub2} + 1$, $P_1 = 3 - L_{sub1} + 1$, respectively, $L_{sub1} = 2$ and $L_{sub2} = 15$ are chosen. Then, the number of subarrays and elements in each sub-array equals to $P = P_1 \times P_2$ and $L = L_{sub1} \times L_{sub2}$. Obviously, the smoothed CSI matrix could provide 32 measurement vectors using one CSI reading only, which makes it feasible to calculate the covariance matrix.

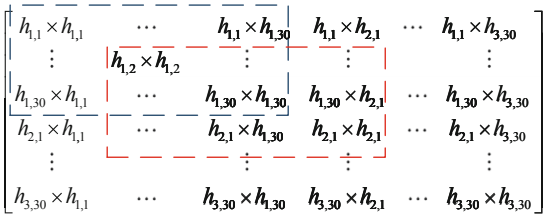

Fig. 3. The virtual array antenna is constructed by Two-dimensional Spatial Smoothing to realize the super resolution estimation of AoA.

The covariance matrix of the CSI after the process of 2D-SS on $\mathbf{R}_U$ is modified into:

$$\mathbf{R}_{2D-SS} = \frac{1}{P_1 \times P_2} \sum_{m=1}^{P_1} \sum_{n=1}^{P_2} \mathbf{R}_{m,n} \tag{7}$$

where $\mathbf{R}_{m,n}$ is the sub-covariance matrix in $\mathbf{R}_U$ with respect to the nth subcarrier at the mth antenna. Then, we conduct the MUSIC algorithm on the smoothed covariance matrix to obtain the direction vectors, as well as the AoA and ToA with respect to each signal path.

3.3 Phase Offsets Compensation and Dynamic Path Signal Extraction

To identify the signal of human reflection path and estimate corresponding AoA, we must compensate for random phase offsets and suppress these strong signal components. Assume the CSI samples without random phase offsets at mth antenna are represented as:

$$H\left(f,\tau,m\right)=\sum_{i=1}^{L}A_i e^{-j2\pi(f+\Delta f_j)\left(\tau_i+\frac{d\sin\beta_{m,i}}{c}\right)} \tag{8}$$

where L represents the total number of multipath, A_i and τ_i represent the complex attenuation factor and propagation time delay of the ith path, f represents the center frequency and Δf_j represents the frequency difference between jth subcarrier and 0th subcarrier, $\beta_{m,i}$ represents the incident angle of the ith path at mth antenna, c is the speed of light. When phase offsets $e^{-j\phi}$ are introduced, the CSI samples are represented as:

$$\begin{cases} H\left(f,\tau,m\right)=e^{-j\phi}\left(\sum\limits_{i=1}^{L}A_i e^{-j2\pi(f+\Delta f_j)\left(\tau_i+\frac{d\sin\beta_{m,i}}{c}\right)}\right) \\ \phi=2\pi\left(k(\lambda_p+\lambda_s)+\Delta t_i\varepsilon_f\right)+\zeta \end{cases} \tag{9}$$

where λ_p and λ_s represent packet detection delay (PDD) and sampling frequency offset (SFO), which are all related to the subcarrier frequency, ε_f represents carrier frequency offset (CFO), k and Δt_i represent the subcarrier index and the packet interval time, respectively. ζ is the initial phase offset between the channels of the receiver, which can be manually corrected by a power splitter as described in [2].

By classifying multipath signals into static group P_s and dynamic group P_d, (9) can be converted into:

$$H\left(f,\tau,m\right)=e^{-j\phi}H_S\left(f\right)+e^{-j\phi}\sum_{i\in P_d}A_i e^{-j2\pi(f+\Delta f_j)\left(\tau_i+\frac{d\sin\beta_{m,i}}{c}\right)} \tag{10}$$

In (10), $f\tau_i$ is the same for all measurements, so it can be merged into the complex attenuation A_i. And $\Delta f_j\tau_i$ (close to 0.0003125) is small enough to be ignored. After omitting the two terms, we have:

$$H\left(f,\tau,m\right)=e^{-j\phi}H_S\left(f\right)+e^{-j\phi}\sum_{i\in P_d}A_i e^{-j2\pi\left(\Delta f_j\tau_i+f\frac{d\sin\beta_{m,i}}{c}\right)} \tag{11}$$

In non-cooperative radar [13], the time domain interference cancellation algorithm, such as batch version of extensive cancellation algorithm (ECA-B), is used to eliminate the direct wave and multipath interference in received signal. The key to this kind of system is to select an independent antenna as a reference antenna to obtain direct wave signals. In Intel 5300 Network Interface Card (NIC) there still contains multiple antennas, and the time-variant random phase offsets are the same across different antennas on a WiFi card [8,10]. To remove random phase offsets, we use the method mentioned in [14,15,22] to calculate the conjugate multiplication of CSI of one pair of antennas. Assume that the reference antenna is the nth one, we get the product of conjugate multiplication:

$$\begin{aligned} H_c\left(f,\tau_i\right) &= H\left(f,\tau,m\right) * \overline{H}\left(f,\tau,n\right) \\ &= \underbrace{H_S\left(f,m\right)\overline{H}_S\left(f,n\right)}_{\text{static term}} + \underbrace{H_S\left(f,m\right)\sum_{l\in Q_d}\overline{B}_l e^{j2\pi\left(\Delta f_j \tau_l + f\frac{d\sin\beta_{n,l}}{c}\right)}}_{\text{target term}} \\ &\quad + \underbrace{\overline{H}_S\left(f,n\right)\sum_{i\in P_d} A_i e^{-j2\pi\left(\Delta f_j \tau_i + f\frac{d\sin\beta_{m,i}}{c}\right)}}_{\text{target term}} \\ &\quad + \underbrace{\sum_{i\in P_d, l\in Q_d} A_i\overline{B}_l e^{-j2\pi\left(\Delta f_j(\tau_i-\tau_l)+f\frac{d\left(\sin\beta_{m,i}-\sin\beta_{n,l}\right)}{c}\right)}}_{\text{cross term}} \end{aligned} \tag{12}$$

where $H\left(f,\tau,m\right)$ is the CSI of the mth antenna, $\overline{H}\left(f,\tau,n\right)$ is the conjugate of CSI of the reference antenna, P_d and Q_d are the sets of dynamic paths at mth antenna and reference one, $\overline{(\cdot)}$ denotes conjugate operation.

More interesting, we find the product (12) can be divided into three categories, named static term, target term and cross term, where the first summation term is static term with lower frequency, which can be treated as a constant in a short time period and can be almost filtered by a high-pass filter. The cross term is only product of dynamic parts on two antennas, which is orders weaker than the others, and can be omitted. The rest is the target term and residual static term, which keep the human location information we care about. In this work, according to a person's normal walking speed (0.3 m/s–2 m/s), we use a bandpass filter to separate out the target term and set the lower and upper cutoff frequencies to 2 Hz and 80 Hz.

We run benchmark experiments to verify the above-mentioned method. We choose a meeting room with a size of 9.0 m × 7.7 m, which is a typical indoor multipath environment. By carefully selecting some test points, it is ensured that the angle of direct path between transceiver is 0° and the resulting reflection path's AoA are located near 45° and 60°. A person spins slightly at these positions to produce reflection signals. We can clearly see in Fig. 5(a) and (d), without the direct wave suppression and de-coherence, the energy peak of the AoA spatial spectrum will appear near around 0°, and the target reflection path's

AoA cannot be detected. While in Fig. 5(b) and (e), after suppressing the direct wave, the AoA of target reflection path appears, but without de-coherence, the spectrum is still blurred. By integrating direct wave suppression and 2D-SS, we can accurately identify the human reflection path's AoA, as shown in Fig. 5(c) and (f). We also introduce Gaussian mean clustering [9] to show the results of multiple experiments, plot in Fig. 4(a) and (b).

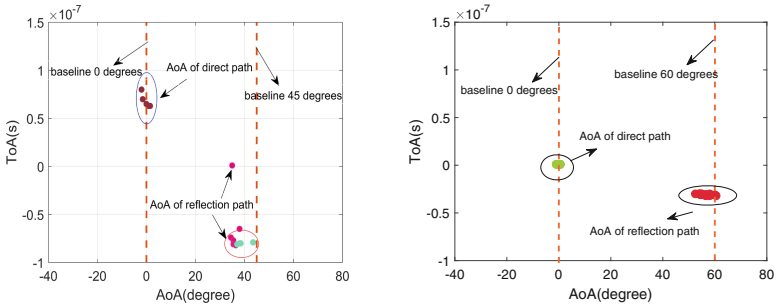

(a) Gaussian mean clustering at 45 degrees.

(b) Gaussian mean clustering at 60 degrees.

Fig. 4. We perform continuous estimation of AoA and plot the clustering result.

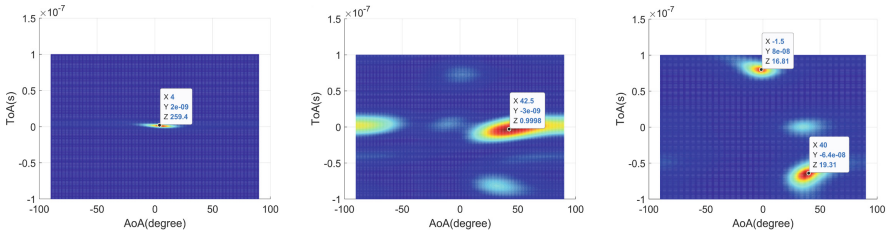

(a) No suppression or smoothing.

(b) With only suppression.

(c) With suppression and smoothing.

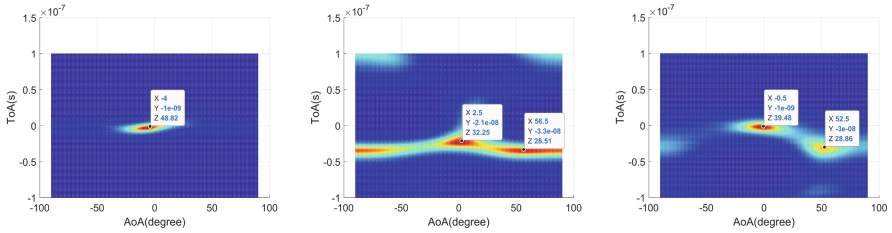

(d) No suppression or smoothing.

(e) With only suppression.

(f) With suppression and smoothing.

Fig. 5. We run benchmark experiments to verify the super-resolution AoA estimation method. Experimental results show the AoA of reflection path can be accurately captured after direct wave suppression and spatial smoothing.

3.4 Target Reflection Path Recognition

The last reflector of the dynamic path is not always the target, we need to separate the human reflection path from all dynamic paths. The AoA of moving human has a larger fluctuation range than other paths in a short time measurement. Similar to the ideas of [3] and [23] and benefit from their inspiration, we believe that the human reflection signal should be the shortest direct dynamic signal with the minimum ToA measurement. Therefore, we rely on the probabilistic analysis to assign a likelihood value to each dynamic path. The likelihood value of each path is calculated by incorporating the number of peak points with the variance of the AoA and ToA.

$$l_k = 1/\left(1 + \exp\left(-\left(\omega_k p_k + \omega_\beta \varsigma_{\beta_k} + \omega_\tau \varsigma_{\tau_k}\right)\right)\right) \tag{13}$$

where p_k, ς_{β_k}, and ς_{τ_k} are the number of peak points and the variance of the AoA and ToA in the cluster corresponding to the kth dynamic path. ω_k, ω_β and ω_τ are the weights of the number of peak points and the variance of the AoA and ToA.

3.5 Target Location Estimation

In this work, human localization is achieved by combining multiple receivers' target AoA information. It is assumed that there are R receivers. Given the receiver locations (x_1, y_1), (x_2, y_2), $\cdots$, (x_R, y_R) and the estimated AoA at each receiver ${\beta_1}^{target}$, ${\beta_2}^{target}$, $\cdots$, ${\beta_R}^{target}$, we need to identify the location $p = (x_p, y_p)$ of the target.

To minimize the deviation between actual values and the observed, we use the least square (LS) criterion [16] and solve the optimal location by minimizing the objective function below.

$$\begin{aligned} &minimize \sum_{i=1}^{R} l_i * {d_i}^2 \\ subject\ to\ \sin\left(\beta_{it}\right) &= \frac{|x_t - x_i|}{\sqrt{\left(x_t - x_i\right)^2 + \left(y_t - y_i\right)^2}} \\ d_i &= e^{j2\pi d \sin\left({\beta_i}^{target}\right) f/c} - e^{j2\pi d \sin(\beta_{it}) f/c} \end{aligned} \tag{14}$$

where the weighting factor l_i is the likelihood value of most likely candidate for the direct human reflection path from ith dynamic path. The basic idea of formulating this optimization problem is searching through all the possible values of the target location and find one that gives the minimum distance from the estimated AoA values. We refer to the method mentioned in [17] and use the modified metric $e^{j2\pi d \sin(\beta_{it}) f/c}$ instead of β_{it}, because it is tolerant to these large errors as the value of the metric remains close even when AoA gets miscalculated from $-90°$ to $90°$.

4 Experimental Evaluation

In this section, we evaluate the performance of WiHlo. We first describe the system implementation and evaluation setup. Then we present detailed experimental results covering overall localization performance, AoA estimation performance and discussion on several factors. Further more, we compare with a typical AoA based system.

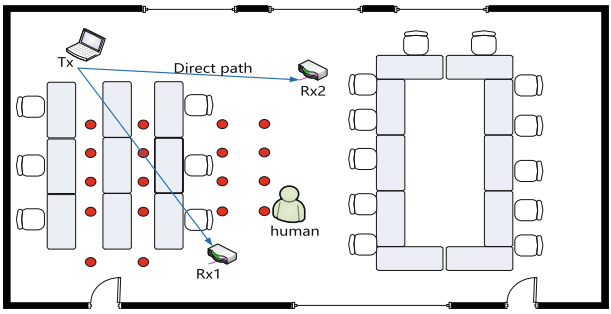

Fig. 6. Meeting room floorplan

4.1 Experimental Methodology

We use a laptop with an omnidirectional antenna to broadcast packets over the air, and two minPCs running Ubuntu 10.04 with an Intel 5300 network interface card (NIC) as receivers. Every receiver has three antennas, forming a uniform linear array. We install the CSI toolkit developed by Halperin [18] on these miniPCs to obtain CSI information for each received packet. Our experiments are conducted in the 5 GHz frequency band with 40 MHz bandwidth, the transmission rate of packets is set to 1 kHz. The processing computer is an ordinary Dell laptop, and processes CSI data using MATLAB. We evaluate system performance in a meeting room, as shown in Fig. 6. The size of the meeting room is 9.0 m× 7.7 m, and there are many chairs and desks which make it a rich multipath scenario. We let a person spin around at those predetermined points noted as red dots in Fig. 6 and use the absolute difference between the measured value and the real one as an indication of error evaluation.

4.2 Localization Performance and AoA Estimation Accuracy

To validate the localization performance of WiHlo, we compare it with MaTrack [8]. Figure 7(a) illustrate the cumulative distribution functions (CDFs) of the localization errors, from the results, we can see that our system outperforms the MaTrack system, specifically, we are able to achieve a median localization error of 0.67 m in the meeting room, while MaTrack's localization accuracy greatly

deviates from the real value, because in this scenario, MaTrack fails to take into account the suppression of strong path signals, resulting in serious inaccurate AoA estimation. Figure 7(b) gives the average AoA estimation performances of WiHlo and the MaTrack, when test in the meeting room, WiHlo achieves a median angle error of 7.5°, such good performance benefits from our phase offsets compensation and direct wave suppression operations.

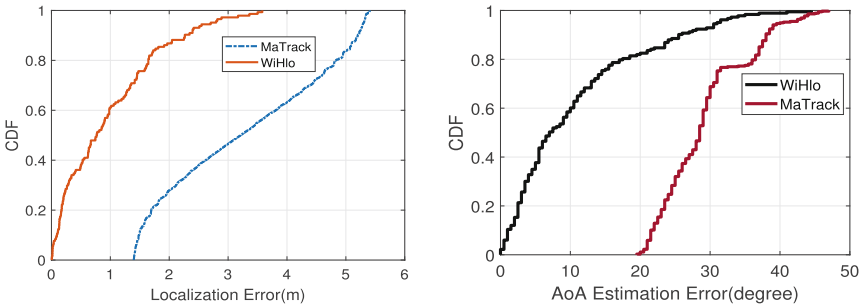

(a) Localization errors. (b) AoA estimation errors.

Fig. 7. We demonstrate the localization accuracy and AoA estimation error of WiHlo and MaTrack.

4.3 Performance Analysis and Discussion

Impact of the Distance Between Transceivers. The distance between the transmitter and receiver affect the system performance, and when the target is in a certain position, the signal-to-noise-ratio (SNR) at a longer distance will be lower. We choose three different distances to verify the impact of the distance between transceivers. Specifically, as shown in Fig. 8(a), the localization error under the transceiver distance of 6 m much larger than 4 m and 2 m. Therefore, we need to select an appropriate transceiver distance according to the size of the monitoring range to ensure the accuracy.

Impact of Packet Rate. In our previous experiment, the packet rate was set at 1 kHz, which put forward high requirements for our WiFi devices since the increase in the packet rate means that the cost and power consumption of the equipment will also increase. In order to verify the effect of different size of packet rate to perception sensitivity, we select several groups of packet rate from small to large to conduct experiments. Figure 8(b) shows the results: Before reaching 500 Hz, the localization accuracy of WiHlo has been improved with the increase of the packet rate. Continuing to improve the packet rate to 2000 Hz has a limited effect on improving the accuracy. Therefore, in order to reduce the requirement for equipment hardware and ensure sufficient accuracy, we can also choose to set the packet rate to 500 Hz.

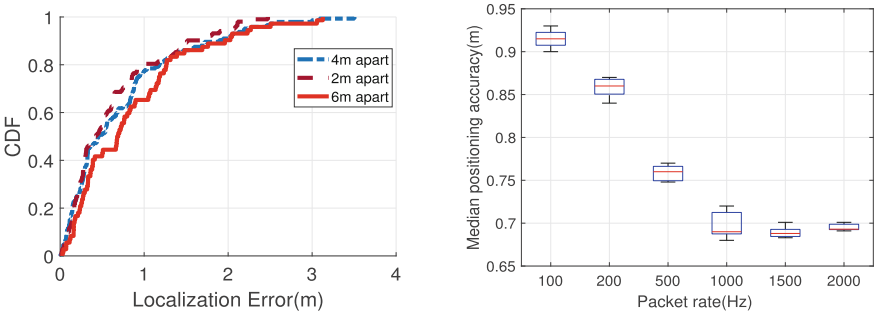

(a) Impact of the distance (b) Impact of packet rate

Fig. 8. We discuss the effects of two factors on localization performance. (a) is the impact of the distance between transceivers; (b) is the impact of packet rate.

5 Conclusion

In this work, we achieve passive localization on commodity WiFi infrastructures. Using the phase offsets compensation and direct wave suppression methods, we separate out the dynamic path. Combining Gaussian mean clustering and probability analysis, we get the AoA of the human reflection path. The experimental results show that our system achieves an average median AoA estimation accuracy of 7.5°, and an average median localization error of 0.67 m under indoor environment, which is better than the existing system.

References

1. Bahl, P., Padmanabhan, V.N.: RADAR: an in-building RF-based user location and tracking system. In: INFOCOM Nineteenth Joint Conference of the IEEE Computer & Communications Societies. IEEE (2000)
2. Xiong, J., Jamieson, K.: ArrayTrack: a fine-grained indoor location system. In: USENIX Conference on Networked Systems Design & Implementation (2013)
3. Kotaru, M., Joshi, K., Bharadia, D., Katti, S.: SpotFi: decimeter level localization using WiFi. ACM SIGCOMM Comput. Commun. Rev. **45**(4), 269–282 (2015)
4. Mao, W., He, J., Qiu, L.: CAT: high-precision acoustic motion tracking. In: International Conference on Mobile Computing & Networking (2016)
5. Adib, F.M., Kabelac, Z., Katabi, D., Miller, R.C.: 3D tracking via body radio reflections (2014)
6. Xu, C., Gao, M., Firner, B., Zhang, Y., Li, J.: Towards robust device-free passive localization through automatic camera-assisted recalibration. In: SenSys (2012)
7. Schmidt, R.: Multiple emitter location and signal parameter estimation. IEEE Trans. Antennas Propag. **34**(3), 276–280 (1986)
8. Li, X., Li, S., Zhang, D., Xiong, J., Wang, Y., Mei, H.: Dynamic-MUSIC: accurate device-free indoor localization. In: ACM International Joint Conference on Pervasive & Ubiquitous Computing (2016)
9. Güngör, E., Özmen, A.: Distance and density based clustering algorithm using Gaussian kernel. Expert Syst. Appl. **69**, 10–20 (2017)

10. Xie, Y., Li, Z., Li, M.: Precise power delay profiling with commodity WiFi. IEEE Trans. Mobile Comput. **PP**(99), 1 (2015)
11. Shan, T.J., Wax, M., Kailath, T.: On spatial smoothing for direction-of-arrival estimation of coherent signals. IEEE Trans. Acoust. Speech Sign. Process. **33**(4), 806–811 (1985)
12. Tian, Z., Li, Z., Zhou, M., Jin, Y., Wu, Z.: PILA: sub-meter localization using CSI from commodity Wi-Fi devices. Sensors **16**(10), 1664 (2016)
13. Wang, J., Wang, H.T., Zhao, Y.: Direction finding in frequency-modulated-based passive bistatic radar with a four-element Adcock antenna array. IET Radar Sonar Navig. **5**(8), 807–813 (2011)
14. Wang, W., Liu, A. X., Shahzad, M., Ling, K., Lu, S.: Understanding and modeling of WiFi signal based human activity recognition. In: International Conference on Mobile Computing & Networking (2015)
15. Qian, K., Wu, C., Zhou, Z., Zheng, Y., Yang, Z., Liu, Y.: Inferring motion direction using commodity Wi-Fi for interactive exergames. In: CHI Conference (2017)
16. Wang, S., Jackson, B.R., Inkol, R.: Hybrid RSS/AOA emitter location estimation based on least squares and maximum likelihood criteria. In: Communications (2012)
17. Bharadia, D., Joshi, K.R., Kotaru, M., Katti, S.: BackFi: high throughput WiFi backscatter. ACM SIGCOMM Comput. Commun. Rev. **45**(5), 283–296 (2015)
18. Halperin, D., Hu, W., Sheth, A., Wetherall, D.: Tool release: gathering 802.11n traces with channel state information. ACM SIGCOMM Comput. Commun. Rev. **41**(1), 53 (2011)
19. Wang, J., Jiang, H., Xiong, J., Jamieson, K., Xie, B.: LiFS: low human-effort, device-free localization with fine-grained subcarrier information. In: International Conference on Mobile Computing & Networking (2016)
20. Xiao, J., Wu, K., Yi, Y., Wang, L., Ni, L.M.: Pilot: passive device-free indoor localization using channel state information (2013)
21. Seifeldin, M., Youssef, M.: Nuzzer: a large-scale device-free passive localization system for wireless environments. IEEE Trans. Mobile Comput. **12**(7), 1321–1334 (2013)
22. Qian, K., Wu, C., Zhang, Y., Zhang, G., Yang, Z., Liu, Y.: Widar2.0: passive human tracking with a single Wi-Fi link. In: Proceedings of the 16th Annual International Conference on Mobile Systems, Applications, and Services (MobiSys 2018), pp. 350–361. ACM, New York (2018). https://doi.org/10.1145/3210240.3210314
23. Zhang, L., Gao, Q., Ma, X., Wang, J., Yang, T., Wang, H.: DeFi: robust training-free device-free wireless localization with WiFi. IEEE Trans. Veh. Technol. **67**(9), 8822–8831 (2018). https://doi.org/10.1109/TVT.2018.2850842
24. Niu, J., Wang, B., Lei, S., Duong, T.Q., Chen, Y.: ZIL: an energy-efficient indoor localization system using ZigBee radio to detect WiFi fingerprints. IEEE J. Sel. Areas Commun. **33**(7), 1431–1442 (2015)
25. Habaebi, M.H., Khamis, R.O., Zyoud, A., Islam, M.R.: RSS based localization techniques for ZigBee wireless sensor network. In: International Conference on Computer & Communication Engineering (2014)
26. Zhu, J., Luo, H., Chen, Z., Li, Z.: RSSI based Bluetooth low energy indoor positioning. In: International Conference on Indoor Positioning & Indoor Navigation (2015)
27. Rida, M.E., Liu, F., Jadi, Y., Algawhari, A.A.A., Askourih, A.: Indoor location position based on Bluetooth signal strength. In: International Conference on Information Science & Control Engineering (2015)